Chemical Science

ROYAL SOCIETY OF CHEMISTRY

EDGE ARTICLE

View Article Online
View Journal | View Issue

Cite this: *Chem. Sci.*, 2020, **11**, 8013

All publication charges for this article have been paid for by the Royal Society of Chemistry

Received 13th May 2020
Accepted 15th July 2020

DOI: 10.1039/d0sc02733b

rsc.li/chemical-science

Selective synthesis and structural transformation between a molecular ring-in-ring architecture and an abnormal trefoil knot†

Li-Long Dang,[a] Xiang Gao,[a] Yue-Jian Lin[a] and Guo-Xin Jin *[ab]

The synthesis of complicated supramolecular architectures and the study of their reversible structural transformations remains a fascinating challenge in the field of supramolecular chemistry. Herein, two types of novel coordination compounds, a non-intertwined ring-in-ring assembly and an abnormal trefoil knot were constructed from a strategically selected Cp*Rh building block and a semi-rigid *N*,*N*′-bis(4-pyridylmethyl)diphthalic diimide ligand *via* coordination-driven self-assembly. Remarkably, the reversible transformation between the abnormal trefoil knot and the ring-in-ring assembly or the corresponding tetranuclear macrocycle could be achieved by the synergistic effects of Ag^+ ion coordination and alteration of the solvent. Single-crystal X-ray crystallographic data and NMR spectroscopic experiments support the structural assignments.

Introduction

In the field of supramolecular chemistry, the aesthetic features and potential applications of interlocked or intertwined compounds continue to motivate scientists to design and construct new compounds with intricate topologies.[1–3] Among the many synthetic strategies applied, coordination-driven self-assembly has proven to be a particularly fruitful approach. Based on this, a wide range of topologies, such as catenanes,[4–7] rotaxanes,[8–13] knots,[14–22] Solomon links,[23–27] Borromean rings,[28–32] and interlocked cages,[33–35] have been constructed. Recent reports of the synthesis and structural transformations of molecular Borromean rings and Solomon links have marked considerable progress in the research field, in particular the development of unlinking transformations from Borromean rings to the corresponding component monomers by taking advantage of the inverse electron-demand Diels–Alder (IEDDA) reaction,[36] and the successful realization of reversible transformation of a Solomon link to an unusual trefoil knot by utilizing the coordination ability of silver(I) ions.[37,38]

Additionally, the successful synthesis of complicated molecular knots,[18,19,39,40] and [*n*]catenanes (*n* = 3, 4, 6)[41–46] are tremendous developments in the study of topologically complex molecules. Nevertheless, structural interconversion between intricate supramolecular architectures is seldom realized due to the difficulties inherent in their design and controllability.[38,47]

Molecular ring-in-ring motif is rarely observed in supramolecular host–guest chemistry, the structures of which are non-intertwined but consist of two chemically independent rings in which one ring encapsulates a second.[48–53] Although an example of a metallarectangle-based molecular ring-in-ring structure has been reported by the group of Chi by using an arene-Ru acceptor and the rigid ligand 1,4-di(pyridin-4-yl)buta-1,3-diyne through π–π interactions,[53] constructing a novel organometallic ring-in-ring complex with a nonrigid ligand and achieving its transformation to other intricate supramolecular structures remains an unfulfilled goal.

In recent works, a series of intricate complexes including molecular trefoil, figure-eight knots and Solomon links have been achieved using the building blocks $[Cp_2^*M_2(\text{BiBzIm})](OTf)_2$ (M = Rh/Ir, BiBzIm = 2,2′-bisbenzimidazole).[21,38] This success was based on the appropriate width and electron deficient characteristics of the BiBzIm plane, which provides the possibility of forming π–π stacking and C–H···π interactions.

In the ligand *N*,*N*′-bis(4-pyridylmethyl)-diphthalic diimide (**L**), the two pyridyl moieties are separated by diimide spacers, and the sp^3-hybridized methylene carbon atoms in **L** allow the two pyridyl arms to rotate freely, thus making ligand **L** an example of a semi-rigid ligand. Moreover, the phthalic diimide (PDM) cores not only bear different angular geometries, but endow the ligand with rich hydrogen-bonding possibilities.[54,55] Additionally, its π-conjugated phthalic diimide and pyridyl moieties can engender favorable aromatic π–π stacking and

[a]*Department of Chemistry, Shanghai Key Laboratory of Molecular Catalysis and Innovative Materials, State Key Laboratory of Molecular Engineering of Polymers, Fudan University, Shanghai 200438, P. R. China*

[b]*State Key Laboratory of Organometallic Chemistry, Shanghai Institute of Organic Chemistry, Chinese Academy of Sciences, Shanghai 200032, P. R. China. E-mail: gxjin@fudan.edu.cn*

† Electronic supplementary information (ESI) available. CCDC 2002844 (**1′**), 2002845 (**2**), 2002846 (**2′**), 2002856 (**2-pyrene**) and 2002847 (**3′**) and 2002843 (**4**). For ESI and crystallographic data in CIF or other electronic format see DOI: 10.1039/d0sc02733b

CH–π interactions. These unique advantages of $[Cp_2^*M_2(\text{-BiBzIm})](OTf)_2$ and ligand **L** provide the possibility of synthesizing novel ring-in-ring assemblies and other supramolecular complex architectures.

Herein, we report the reversible structural transformation between a molecular ring-in-ring complex and an abnormal trefoil knot for the first time, which can be achieved by the addition or removal of Ag^+ ions. And these two structures can also transform to the corresponding tetranuclear macrocycle based on solvent effects and/or the presence of Ag^+ ions. These three compounds are synthesised by coordination-driven self-assembly of the $[Cp_2^*Rh_2(BiBzIm)](OTf)_2$ building block and a semi-rigid diimide ligand (**L**) under mild conditions. π–π and C–H···π interactions may play synergetic roles in the formation of the ring-in-ring assembly and abnormal trefoil knot. In addition, these structures and their reversible transformation are unambiguously characterized by NMR spectroscopy, ESI-MS, and single-crystal X-ray diffraction analysis.

Results and discussion

Self-assembly of tetranuclear macrocycle 1 and ring-in-ring complex 2

The reaction of $[Cp_2^*Rh_2(BiBzIm)](OTf)_2$ (**E1**) with AgOTf (2.0 equiv.) in CH_3CN, followed by the addition of **L**, produced a tetranuclear macrocycle complex **1** (yield: 88%; Scheme 1). The structure of **1** was confirmed by NMR spectroscopy (Fig. S6–S9, ESI†) and X-ray crystallographic analysis (Fig. 1).

The ^{1}H NMR spectrum of **1** in CD_3CN showed doublets at δ 8.26, 7.67 and 7.07 ppm and two singlets at δ 7.86 and 4.33 ppm corresponding to the protons of **L**, while the protons of BiBzIm appeared as two multiplet peaks at δ 7.93–7.94 and 7.42–7.44 ppm (Fig. S6, ESI†). The ^{1}H DOSY NMR spectrum of **1** showed a single diffusion coefficient ($D = 5.04 \times 10^{-10}$ m^2 s^{-1}), suggesting that only one stoichiometry of assembly was formed (Fig. S8, ESI†). The structure of **1** in solution was also supported by ESI-MS. The prominent signal at m/z = 838.16 ($[\mathbf{1}–3OTf^-]^{3+}$) is in good agreement with the theoretical isotopic distribution

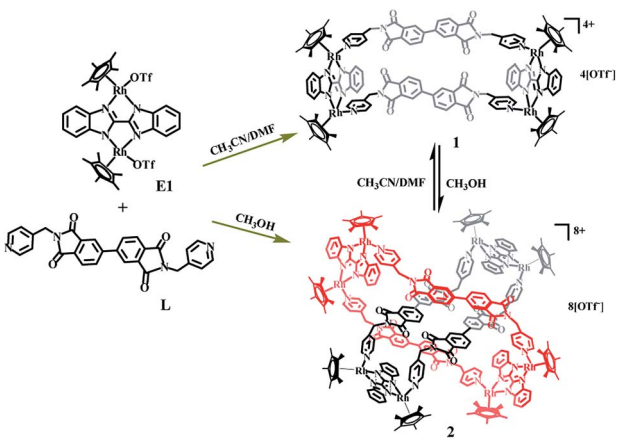

Scheme 1 Self-assembly of tetranuclear complex **1** and ring-in-ring structure **2**.

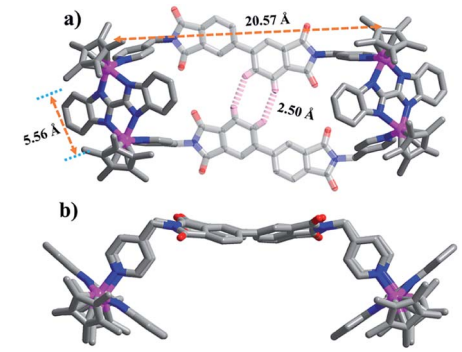

Fig. 1 Single-crystal X-ray structure of **1′**: (a) top view, (b) side view. Most hydrogen atoms, anions, solvent molecules and disordered elements are omitted for clarity (N, blue; O, red; C, gray; Ir, pink).

(Fig. 2A). In addition, only a single complex was detected in solution in a wide range of concentrations, suggesting the significant stability of **1** in CD_3CN (Fig. S10, ESI†).

To gain further information regarding complex **1**, NMR spectroscopic experiments were carried out in $[D_7]$-DMF solution (30.0 mM, with respect to Cp*Rh). The ^{1}H NMR spectrum of the solution presented similar signals to those observed in CD_3CN solution, indicating that **1** is similarly stable in $[D_7]$-DMF solution (Fig. S11, ESI†).

The Cp*Ir-based complex **1′** was prepared analogously to **1** by combination of **E1′** and **L** in a yield of 83% and was crystallised by diffusion of diethyl ether into its acetonitrile solution. **1′** was found to be a boat-shaped tetranuclear macrocycle by single-crystal X-ray diffraction analysis (Fig. 1). The two binuclear (Ir^{III}) molecular clips (**E1′**) are linked by two dipyridyl ligands, adopting *U*-conformations with dimensions of 5.56 Å (short Ir···Ir nonbonding distances) and 20.57 Å (long Ir···Ir nonbonding distances). The shortest H–H distance between two adjacent PDM of different **L** units is *ca.* 2.50 Å. This small internal space of the tetranuclear macrocycle **1** presumably hampers the formation of interlocked metallarectangles or other more complicated species.

In an effort to perturb the synthesis of **1** through solvent alteration, ligand **L** was added to a CH_3OH solution of **E1**, and the mixture was stirred for 8 h, resulting in a yellow solution.

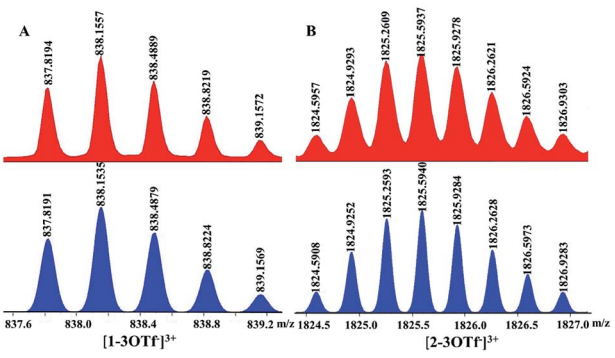

Fig. 2 Calculated (bottom, blue) and experimental (top, red) ESI-MS spectra (3^+) of (A) tetranuclear **1** and (B) ring-in-ring complex **2**.

Then, a 1 : 1 mixture of methanol and isopropyl ether as transition layer solution was gradually added to the above solution until the transition layer became colorless. After that, an equivalent volume of isopropyl ether was added. Single crystals **2** suitable for X-ray diffraction were obtained from this mixture in 82% yield after 3 days (Fig. 3).

The solid-state structure of **2** shows that complex **2** has a non-catenane interlocked structure in which one macrocyclic unit threads another (chemical) identical macrocycle, thus forming a ring-in-ring complex. Close-contact analysis of the structure shows that the individual macrocycle forms a chair-shaped structure composed of two binuclear molecular clips **E1** linked by two pyridyl ligands with *Z*-conformations. However, the phthalic diimide moieties in each macrocycle reveal different conformations (horizontal and parallel). The horizontal arrangement of adjacent phthalic diimide moieties in the outer macrocycle results in a distance that is wide enough to accommodate another macrocycle (minimum distance (r(H···O)): 5.1 Å), while the parallel arrangement of the inner macrocycle makes this unit narrower. The ring-in-ring structure is stabilized by parallel-displaced π–π interactions (of interlayer distance 3.59 Å) between the pyridyl moieties and phthalic diimide moieties of two macrocycles, as well as edge-to-face-type CH–π interactions (2.76 Å) between the BiBzIm moieties and the phenyl groups of the phthalic diimide ligands. In addition, the presence of four weak C–H···O hydrogen bonds[56,57] (distances r(H···O) = 2.48–2.69 Å and angles ∠COH = 136.21–155.87°) suggest that inter-macrocycle interactions between the phthalic diimide moieties might also play a pivotal role in stabilizing the ring-in-ring structure (Fig. 2). Moreover, the analogous Cp*Ir-based ring-in-ring complex **2′** was separately constructed in a yield of 87%.

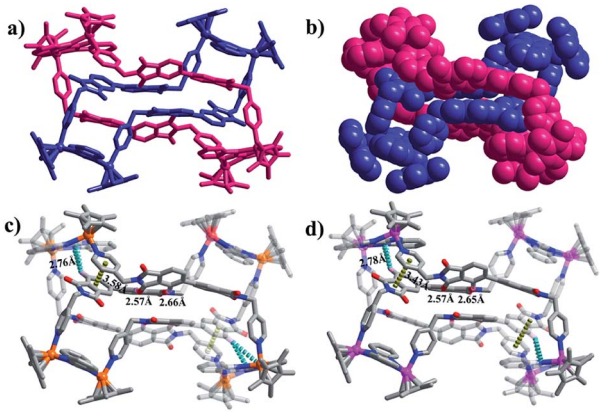

Fig. 3 (a) Wireframe, and (b) space-filling representations of the solid-state structure of ring-in-ring complex **2** coloured according to ring; (c) wireframe representation of the solid-state structure of ring-in-ring complex **2** coloured according to atom; (d) wireframe representation of the solid-state structure of ring-in-ring complex **2′** coloured according to atom. Measurements in (c and d) indicate π–π stacking interactions between PDM groups and pyridine moieties and CH···π interactions between BiBzIm moieties and phenyl moieties of PDM groups. Hydrogen atoms, anions, solvent molecules and disorder are omitted for clarity (atom colours: N, blue; O, red; C, gray; Rh, orange; Ir, pink).

After determination of the solid-state molecular structure of ring-in-ring complex **2**, extensive attempts were made to explore its behavior in solution by NMR spectroscopy, however, these were significantly hampered by the very poor solubility of complex **2** in CD_3OD. However, the ESI-MS spectrum of **2** indicated that the ring-in-ring dimeric structure of the complex is retained in solution: $[\mathbf{2}–3\mathrm{OTf}]^{3+}$ (m/z = 1825.59) (Fig. 2B). Additionally, the poor solubility of **2** might reflect the compactness of its ring-in-ring architecture.

A recent series of works have revealed that pyrene can induce the reversible conversion of some interlocked metallacycles to non-catenane rectangles through the inclusion of the former as a guest molecule.[6,58] To investigate the inductive effect of pyrene on the dimeric ring-in-ring structure, a similar self-assembly reaction of **E1** and **L** in the presence of pyrene was performed, resulting in the new complex **2-pyrene**. The single-crystal X-ray analysis of **2-pyrene** shows that the pyrene molecules are distributed around the ring-in-ring structure by forming π–π stacking interactions with the Cp* groups or as free guest molecules, clearly indicating that the pyrene molecules are unable to separate the macrocycles of the ring-in-ring structure (Fig. 4).

Self-assembly of abnormal trefoil knots 3 and 3′

As reported previously, the building block $[Cp_2{*}Ir_2(\text{-BiBzIm})](OTf)_2$ (**E1′**) can react with two Ag^+ ions and a BiBzIm ligand to form the Ag^+-ions-bridged complex **E3** based on the formation of N–Ag–N bonds,[38] and **E1′** can also be re-formed by removal of Ag^+ ions by sunlight or Cl^- ions, thus providing a reliable method for adjusting the size of the building block. This strategy encouraged us to explore whether the introduction of Ag^+ ions into the ring-in-ring system could result in its supramolecular transformation. Thereby, a mixture of silver triflate and BiBzIm was added during the self-assembly process of complex **2**. The resulting mixture was stirred for 6 h in the dark at room temperature, at which point evaporation of solvent and recrystallization provided compound **3** as a yellow solid (yield: 89%). In addition, the analogous **E3**-based complex **3′** was separately constructed in a yield of 90% (Scheme 2). The structures of **3** and **3′** were confirmed by NMR spectroscopy, ESI-MS, and single-crystal X-ray diffraction analysis.

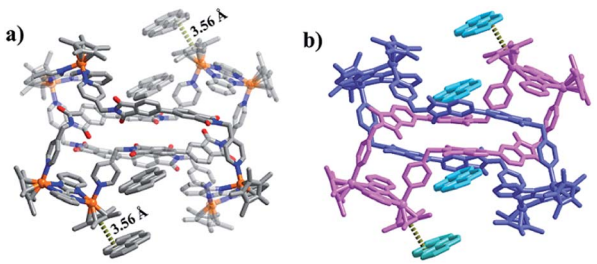

Fig. 4 Wireframe representation of solid-state structure of **2-pyrene** coloured according to (a) atom and (b) ring. Hydrogen atoms, anions, solvent molecules and disorder are omitted for clarity (atom colours: N, blue; O, red; C, gray; Rh, orange).

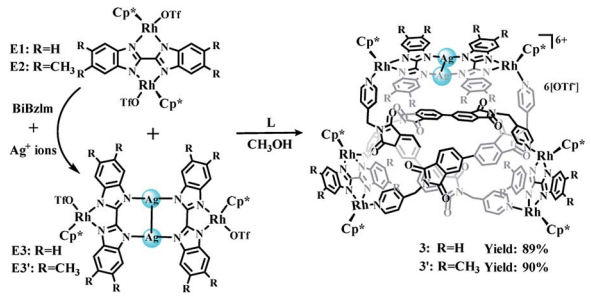

Scheme 2 Self-assembly of abnormal trefoil knots **3** and **3′**.

Complex **3** exhibited a far greater solubility in CH_3OH than complex **2**. Therefore, the relevant NMR spectroscopic experiments in CD_3OD were performed to explore its solution behavior. The ^{1}H NMR spectrum (Fig. S17, ESI†) of **3** shows very complicated peaks which can be analyzed by combination with ^{1}H–^{1}H COSY NMR (Fig. S18, ESI†), ^{1}H DOSY NMR spectra (Fig. S19, ESI†) and ^{1}H–^{13}C HSQC NMR (Fig. S21, ESI†) of **3**. The ^{1}H NMR spectrum shows three singlets at δ 1.79, 1.66 and 1.50 ppm in a ratio of 1 : 1 : 1, which can be attributed to three types of Cp* groups, reflecting the formation of a new compound with an intricate structure. It also showed six doublets at δ 5.17, 4.51, 4.40, 4.34, 4.17 and 3.84 ppm for the protons of –CH_2– groups of **L** ligands. Another three singlets at δ 7.86, 6.75, 5.95 ppm and five doublets at 5.08, 5.06, 4.59, 4.15, 3.81 ppm display the protons of PDM groups of **L** ligands. Besides, there are two multiplet peaks at δ 8.80–8.77 and 7.37–7.33 ppm, corresponding to the protons of pyridyl groups of ligands **L**. The prominent doublets at δ 8.43, 8.20, 8.12, 8.07, 7.93, 7.19 ppm, triplets at δ 7.51, 7.03 ppm could be attributed to multiple types of **BiBzIm** groups. In addition, the ^{1}H DOSY NMR spectrum of **3** shows that the aromatic and Cp* signals are associated with a single diffusion constant ($D = 2.36 \times 10^{-10}$ m^2 s^{-1}), suggesting that only one stoichiometry of assembly is formed in methanol (Fig. S19, ESI†). Along with this NMR spectroscopic data, ESI-MS also indicated the presence of complex **3** in solution: $[\mathbf{3}–2OTf^-]^{2+}$ (m/z = 2296.23) and $[\mathbf{3}–3OTf^-]^{3+}$ (m/z = 1480.84) (Fig. 5). The abnormal trefoil knot topology of **3** in the solid state was confirmed by single-crystal X-ray analysis. However, despite great efforts, the crystal data of **3** is not ideal (Fig. S3†).

Fortunately, single crystals more suitable for X-ray diffraction were obtained by slow vapor diffusion of diethyl ether into a saturated solution of **3′** in CH_3OH under ambient conditions for four days. The structure was definitively revealed by X-ray crystallographic analysis to have an abnormal trefoil knot topology. Complex **3′** crystallises in space group *C*2/*c* with the topology of a 3_1 knot according to the Alexander–Briggs notation. The observation of a 1 : 1 ratio of both enantiomers (ΛΛΛ and ΔΔΔ) is consistent with other reported trefoil knot structures[16] (Fig. 6c and d). In the refined structure, two different binuclear units are connected *via* ligands **L** featuring two different geometries (*U* and *Z* shapes), making up an abnormal trefoil knot form. The diagonal centroid–centroid distance of benzene groups of the newly-formed Ag(I)-containing bridging building block **E3′** (10.40 Å) is similar to the separation of two nitrogen-atoms of phthalic diimide groups of **L** (10.59 Å), which allows for the face-to-face placement of phthalic diimide groups of **L** and the benzene rings of **E3′**. The distances between phthalic diimide groups of **L** and the opposing benzene rings of **E3′** are *ca.* 3.66 and 3.93 Å, indicating the formation of π–π interactions between the TmBiBzIm group of **E3′** and **L**. Edge-to-face-type CH···π interactions (*ca.* 2.46, 2.68 Å) between the phenyl moieties of **L** and TmBiBzIm were observed, in addition to parallel-displaced π–π interactions (of interlayer distance 3.77 Å) between benzene rings and adjacent pyridyl moieties of another **L** (Fig. S2, ESI†). Thus it is likely that the stabilization of the abnormal trefoil knot structure is due to a combination of π–π and CH···π interactions (Fig. 6a and b). As the abnormal trefoil knot structure of **3′** is achieved by the formation of only one Ag(I)-containing bridging building block **E3′** with the two other **E3** building blocks remaining Ag(I)-free, we wondered if additional Ag(I) ions would result in further structural

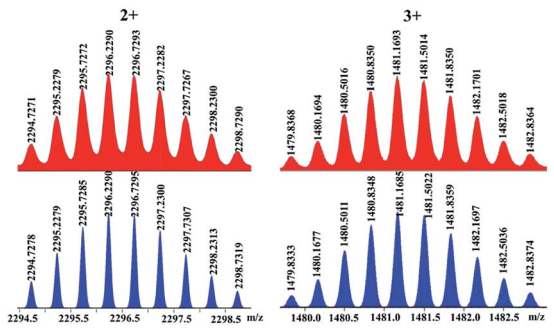

Fig. 5 Calculated (bottom, blue) and experimental (top, red) ESI-MS spectra of **3**.

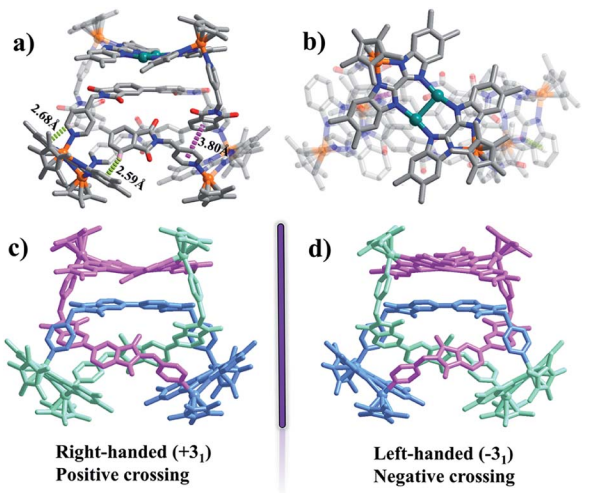

Fig. 6 Molecular structure of **3′** coloured according to atom: (a) top view; (b) side view. Wireframe representation of (c) right-handed trefoil knot ($+3_1$) of **3′** and (d) left-handed trefoil knot (-3_1) of **3′**. Counter-anions and hydrogen atoms are omitted for clarity (atom colours: N, blue; O, red; C, gray; Ag, teal; Rh, orange).

transformation of **3′** to other intricate structures. In a series of exploratory experiments, different amounts of silver(I) triflate were added to solutions of **3′** in CH_3OH. However, in all of these experiments, only the abnormal trefoil knot **3′** was observed by NMR spectroscopy (Fig. S22–S24†), ESI-MS (Fig. S38†), and single-crystal X-ray crystallographic analysis.

Structural transformations between abnormal trefoil knot 3 and ring-in-ring complex 2 or tetranuclear macrocycle 1

The solvent-dependent formation of tetranuclear macrocycle and ring-in-ring complexes encouraged us to explore their interconversion starting from the respective pure entities. We speculated that alteration of the solvent might promote a unique and reversible conversion between ring-in-ring complex **2** and tetranuclear rectangle **1**. Upon dissolution of crystals of the ring-in-ring complex **2** in CD_3CN, a set of simple ^{1}H NMR spectroscopic signals was observed, clearly indicating the formation of tetranuclear rectangle **1**. The initial ^{1}H NMR spectrum of tetranuclear rectangle **1** in CD_3OD also showed simple peaks, however, over time, precipitation began to appear along with the reduction of the intensity of the ^{1}H NMR signals. Accordingly, we grew single crystals of this species by slow vapor diffusion of diethyl ether into a saturated solution of **1** in CH_3OH under ambient conditions. X-ray crystallographic data obtained for these crystals were consistent with those of **2**, confirming the ability of complex **1** to convert gradually to a ring-in-ring complex in CH_3OH (Scheme 3).

Meanwhile, upon addition of AgOTf (2.0 equiv.) to a turbid solution of ring-in-ring complex **2** in CD_3OD, the solid gradually dissolved and a complicated set of ^{1}H NMR signals appeared, that were consistent with the ^{1}H NMR spectrum of complex **3**, confirming the transformation from ring-in-ring complex to an abnormal trefoil knot. Likewise, upon combining AgOTf (2.0 equiv.) and tetranuclear rectangle **1** in CD_3OD, clear changes in the ^{1}H NMR spectra were observed that indicated the gradual transformation from tetranuclear rectangle to an abnormal trefoil knot.

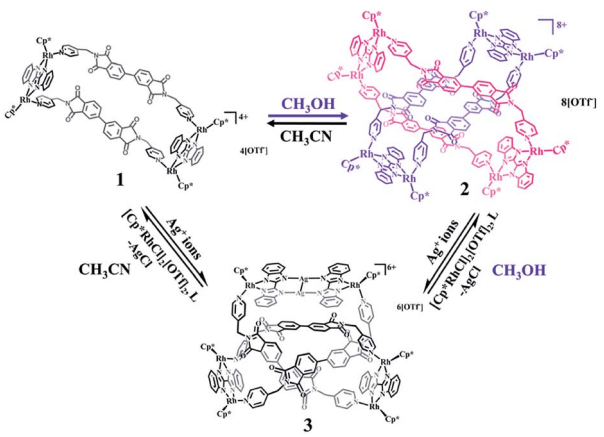

Scheme 3 Schematic representation of supramolecular transformations between tetranuclear macrocycle **1**, ring-in-ring complex **2** and abnormal trefoil knot **3** induced by the chemical reactivity of Ag^+ ions and solvent effects.

It is well documented that Ag^+ ions are extremely sensitive toward light and can react with Cl^- ions to form insoluble precipitates in solution. This opened the possibility of transformation between the silver-containing abnormal trefoil knots and ring-in-ring architectures or tetranuclear rectangles either by exposure to sunlight or addition of Cl^- ions. As expected, in CH_3OH, trefoil knot **3** transformed smoothly into ring-in-ring architecture **2** upon removal of both Ag(I) ions by exposure to with sunlight, which was additionally supported by X-ray crystallographic analysis. Correspondingly, adding $[Cp^*RhCl_2]_2$, AgOTf and **L** in appropriate amounts to a methanol solution of **3** also led to formation of the ring-in-ring complex. Thereby, light-induced degradation led to removal of the Ag(I) ions in complex **3**, providing a clear yellow solution after filtration to which silver triflate (4.0 equiv.), $[Cp^*RhCl_2]_2$ (1.0 equiv.) and ligand **L** (1.0 equiv.) were added. Single crystals suitable for X-ray diffraction were subsequently obtained by slow vapor diffusion of diethyl ether into the yellow solution under ambient conditions for three days. The structure was confirmed to be ring-in-ring structure **2**. In another reaction, silver triflate (2.0 equiv.) was added to a solution of $[Cp^*RhCl_2]_2$ (1.0 equiv.) in CH_3OH in the dark, at which point ligand **L** (1.0 equiv.) and complex **3** (1.0 equiv.) were added to the filtered solution. A yellow solution was acquired after 12 h. Subsequently, single-crystal X-ray crystallography confirmed this species to be the ring-in-ring complex **2**. Additionally, a similar experimental process were also attempted in CH_3CN, providing compound **1**, confirming that the removal of silver ions with sunlight or Cl^- ions can facilitate the transformation of trefoil knot **3** to macrocycle **1** in CH_3CN. This results provide the first confirmation of interconversion between ring-in-ring, trefoil knot and tetranuclear rectangle architectures, which is an important milestone for the development of field of supramolecular chemistry.

Conclusions

In summary, we have demonstrated a selective and reversible transformation between molecular ring-in-ring structures and abnormal trefoil knots for the first time by addition of Ag^+ ions under ambient condition. Both structures were further proven to be convertible to the corresponding tetranuclear macrocycle. New molecular ring-in-ring structures, abnormal trefoil knots and tetranuclear macrocycles bearing semi-rigid ligands were synthesised in high yields, and these structures were confirmed by X-ray crystallographic analysis, NMR spectroscopy and ESI-MS. π–π stacking and C–H···π interactions were shown to play important roles in the stabilization of the ring-in-ring and abnormal trefoil knot architectures. A deeper understanding of supramolecular transformations induced by the addition and removal of Ag^+ ions reaction and solvent effects will be helpful to construct bespoke architectures and responsive supramolecular systems, opening up new insights into the field of smart materials.

Conflicts of interest

There are no conflicts to declare.

Acknowledgements

This work was supported by the National Science Foundation of China (21531002, 21720102004) and the Shanghai Science Technology Committee (19DZ2270100).

Notes and references

1 R. S. Forgan, J.-P. Sauvage and J. F. Stoddart, *Chem. Rev.*, 2011, **111**, 5434–5464.
2 T. R. Cook and P. J. Stang, *Chem. Rev.*, 2015, **115**, 7001–7045.
3 W. L. Shan, Y. J. Lin, F. E. Hahn and G.-X. Jin, *Angew. Chem., Int. Ed.*, 2019, **58**, 5882–5886.
4 J. F. Nierengarten, C. O. Dietrich-Buchecker and J.-P. Sauvage, *J. Am. Chem. Soc.*, 1994, **116**, 375–376.
5 N. H. Evans and P. D. Beer, *Chem. Soc. Rev.*, 2014, **43**, 4658–4683.
6 H. Lee, P. Elumalai, N. Singh, H. Kim, S. U. Lee and K. W. Chi, *J. Am. Chem. Soc.*, 2015, **137**, 4674–4677.
7 X.-Y. Chang, G.-T. Xu, B. Cao, J.-Y. Wang, J.-S. Huang and C.-M. Che, *Chem. Sci.*, 2017, **8**, 7815–7820.
8 T. B. Gasa, C. Valente and J. F. Stoddart, *Chem. Soc. Rev.*, 2011, **40**, 57–78.
9 J. E. M. Lewis, R. J. Bordoli, M. Denis, C. J. Fletcher, M. Galli, E. A. Neal, E. M. Rochette and S. M. Goldup, *Chem. Sci.*, 2016, **7**, 3154–3161.
10 T. H. Ngo, J. Labuta, G. N. Lim, W. A. Webre, F. D'Souza, P. A. Karr, J. E. M. Lewis, J. P. Hill, K. Ariga and S. M. Goldup, *Chem. Sci.*, 2017, **8**, 6679–6685.
11 E. M. G. Jamieson, F. Modicom and S. M. Goldup, *Chem. Soc. Rev.*, 2018, **47**, 5266–5311.
12 M. Gaedke, F. Witte, J. Anhauser, H. Hupatz, H. V. Schroder, A. Valkonen, K. Rissanen, A. Lutzen, B. Paulusa and C. A. Schalley, *Chem. Sci.*, 2019, **10**, 10003–10009.
13 A. W. Heard and S. M. Goldup, *Chem*, 2020, **6**, 994–1006.
14 C. O. Dietrich-Buchecker and J.-P. Sauvage, *Angew. Chem., Int. Ed.*, 1989, **28**, 189–192.
15 N. Ponnuswamy, F. B. L. Cougnon, G. D. Pantos and J. K. M. Sanders, *J. Am. Chem. Soc.*, 2014, **136**, 8243–8251.
16 S. D. P. Fielden, D. A. Leigh and S. L. Woltering, *Angew. Chem., Int. Ed.*, 2017, **56**, 11166–11194.
17 J.-P. Sauvage, *Angew. Chem., Int. Ed.*, 2017, **56**, 11080–11093.
18 L. Zhang, A. J. Stephens, A. L. Nussbaumer, J. F. Lemonnier, P. Jurček, I. J. Vitorica-Yrezabal and D. A. Leigh, *Nat. Chem.*, 2018, **10**, 1083–1088.
19 J. J. Danon, D. A. Leigh, S. Pisano, A. Valero and I. J. Vitorica-Yrezabal, *Angew. Chem., Int. Ed.*, 2018, **130**, 14029–14033.
20 L. Zhang, A. J. Stephens, J. F. Lemonnier, L. Pirvu, I. J. Vitorica-Yrezabal, C. J. Robinson and D. A. Leigh, *J. Am. Chem. Soc.*, 2019, **141**, 3952–3958.
21 L.-L. Dang, Z.-B. Sun, W.-L. Shan, Y.-J. Lin, Z.-H. Li and G.-X. Jin, *Nat. Commun.*, 2019, **10**, 2057.
22 Y. Segawa, M. Kuwayama, Y. Hijikata, M. Fushimi, T. Nishihara, J. Pirillo, J. Shirasaki, N. Kubota and K. Itami, *Science*, 2019, **365**, 272–276.
23 M. Fujita and K. Ogura, *Coord. Chem. Rev.*, 1996, **148**, 249–264.
24 F. Ibukuro, M. Fujita, K. Yamaguchi and J.-P. Sauvage, *J. Am. Chem. Soc.*, 1999, **121**, 11014–11015.
25 N. H. Evans and P. D. Beer, *Chem. Soc. Rev.*, 2014, **43**, 4658–4683.
26 C. Schouwey, J. J. Holstein, R. Scopelliti, K. O. Zhurov, K. O. Nagornov, Y. O. Tsybin, O. S. Smart, G. Bricogne and K. Severin, *Angew. Chem., Int. Ed.*, 2014, **53**, 11261–11265.
27 Y. H. Song, N. Singh, J. Jung, H. Kim, E. H. Kim, H. K. Cheong, Y. Kim and K. W. Chi, *Angew. Chem., Int. Ed.*, 2016, **55**, 2007–2011.
28 J. C. Loren, M. Yoshizawa, R. F. Haldimann, A. Linden and J. S. Siegel, *Angew. Chem., Int. Ed.*, 2003, **42**, 5702–5705.
29 K. S. Chichak, S. J. Cantrill, A. R. Pease, S.-H. Chiu, G. W. V. Cave and J. L. Atwood, *Science*, 2004, **304**, 1308–1312.
30 Y. Lu, Y.-X. Deng, Y.-J. Lin, Y.-F. Han, L.-H. Weng, Z.-H. Li and G.-X. Jin, *Chem*, 2017, **3**, 110–121.
31 C. A. Schalley, *Angew. Chem., Int. Ed.*, 2004, **43**, 4399–4401.
32 L. Zhang, L. Lin, D. Liu, Y. J. Lin, Z. H. Li and G.-X. Jin, *J. Am. Chem. Soc.*, 2017, **139**, 1653–1660.
33 M. Fujita, N. Fujita, K. Ogura and K. Yamaguchi, *Nature*, 1999, **400**, 52–55.
34 M. Fukuda, R. Sekiya and R. Kuroda, *Angew. Chem., Int. Ed.*, 2008, **47**, 706–710.
35 A. Mishra, A. Dubey, J. W. Min, H. Kim, P. J. Stang and K. W. Chi, *Chem. Commun.*, 2014, **50**, 7542–7544.
36 W.-X. Gao, H.-J. Feng, Y.-J. Lin and G.-X. Jin, *J. Am. Chem. Soc.*, 2019, **141**, 9160–9164.
37 H.-J. Feng, W.-X. Gao, Y.-J. Lin and G.-X. Jin, *Chem.–Eur. J.*, 2019, **25**, 14785–14789.
38 H.-N. Zhang, W.-X. Gao, Y.-J. Lin and G.-X. Jin, *J. Am. Chem. Soc.*, 2019, **141**, 16057–16063.
39 J. J. Danon, A. Krüger, D. A. Leigh, J. F. Lemonnier, A. J. Stephens, I. J. Vitorica-Yrezabal and S. L. Woltering, *Science*, 2017, **355**, 159–162.
40 Y. Inomata, T. Sawada and M. Fujita, *Chem*, 2020, **6**, 294–303.
41 R. Zhu, J. Lübben, B. Dittrich and G. H. Clever, *Angew. Chem., Int. Ed.*, 2015, **54**, 2796–2800.
42 C. S. Wood, T. K. Ronson, A. M. Belenguer, J. J. Holstein and J. R. Nitschke, *Nat. Chem.*, 2015, **7**, 354–358.
43 J. Singh, D. H. Kim, E. H. Kim, N. Singh, H. Kim, R. Hadiputra, J. Jung and K. W. Chi, *Chem. Commun.*, 2019, **55**, 6866–6869.
44 T. Sawada, Y. Inomata, K. Shimokawa and M. Fujita, *Nat. Commun.*, 2019, **10**, 5687.
45 J. Singh, D. H. Kim, E. H. Kim, H. Kim, R. Hadiputra, J. Jung and K. W. Chi, *J. Am. Chem. Soc.*, 2020, **142**, 9327–9336.
46 T. Feng, X. Li, Y. Y. An, S. Bai, L. Y. Sun, Y. Li, Y. Y. Wang and Y. F. Han, *Angew. Chem., Int. Ed.*, 2020, DOI: 10.1002/anie.202004112.
47 L.-L. Dang, X. Gao, Y.-J. Lin and G.-X. Jin, *Chem. Sci.*, 2020, **11**, 1226–1232.
48 M. Schmittel, A. Ganz and D. Fenske, *Org. Lett.*, 2002, **4**, 2290–2292.
49 R. S. Forgan, D. C. Friedman, C. L. Stern, C. J. Bruns and J. F. Stoddart, *Chem. Commun.*, 2010, **46**, 5861–5863.

50 J. K. Klosterman, J. Veliks, D. K. Frantz, Y. Yasui, M. Loepfe, E. Zysman-Colman, A. Linden and J. S. Siegel, *Org. Chem. Front.*, 2016, **3**, 661–666.
51 M. C. Lipke, T. Cheng, Y. L. Wu, H. Arslan, H. Xiao, M. R. Wasielewski, W. A. Goddard and J. F. Stoddart, *J. Am. Chem. Soc.*, 2017, **139**, 3986–3998.
52 K. Cai, M. C. Lipke, Z. C. Liu, J. Nelson, T. Cheng, Y. Shi, C. Y. Cheng, D. K. Shen, J. M. Han, S. Vemuri, Y. N. Feng, C. L. Stern, W. A. Goddard, M. R. Wasielewski and J. F. Stoddart, *Nat. Commun.*, 2018, **9**, 5275.
53 V. Vajpayee, Y. H. Song, T. R. Cook, H. Kim, Y. Lee, P. J. Stang and K. W. Chi, *J. Am. Chem. Soc.*, 2011, **133**, 19646–19649.
54 X.-Q. Lü, J.-J. Jiang, L. Zhang, C.-L. Chen, C.-Y. Su and B.-S. Kang, *Cryst. Growth Des.*, 2005, **5**, 419–421.
55 Q.-X. Cheng, J.-J. Lan, Y.-Q. Chen, J. Lin, R. C. K. Reddy, X. M. Lin and Y.-P. Cai, *Inorg. Chem. Commun.*, 2018, **96**, 30–33.
56 M. Fourmigué and P. Batail, *Chem. Rev.*, 2004, **104**, 5379–5418.
57 X. G. Yang, X. M. Lu, Z. M. Zhai, Y. Zhao, X. Y. Liu, L. F. Ma and S. Q. Zang, *Chem. Commun.*, 2019, **55**, 11099–11102.
58 T. Kim, N. Singh, J. Oh, E. H. Kim, J. Jung, H. Kim and K. W. Chi, *J. Am. Chem. Soc.*, 2016, **138**, 8368–8371.